Pergamon

Int. J. Solids Structures Vol. 35, No. 15, pp. 1723–1741, 1998

0020–7683/98 $19.00 + .00

PII: S0020–7683(97)00137–6

DAMAGE OF MASONRY PANELS REINFORCED BY FRP SHEETS

R. LUCIANO and E. SACCO
Dipartimento di Ingegneria Industriale, Università di Cassino, Via Zambosh 43, 03043 Cassino, Italy
E-mail: sacco@ing.unicas.it

(*Received* 24 *July*, 1996; *in revised form* 15 *May* 1997)

Abstract—In this paper the mechanical behavior of a masonry wall is studied. The masonry is regarded as a composite realized by a regular arrangement of blocks into a matrix of mortar. Hence, a panel of masonry is a three-dimensional heterogeneous body with a finite thickness and R^2-periodicity in the plane of the wall. A micromechanical approach is proposed to get the overall properties of the masonry. Then, a case of a wall reinforced by FRP-layered sheets placed on the surfaces of the wall is analyzed. To model the overall behavior of the unreinforced and reinforced masonry, by accounting for the progressive damage of the mortar, of the block and of the FRP sheets, a simple homogenization technique is proposed. Two different damage criteria are adopted for the mortar and the block, within isotropic viscoelastic and elastic damage models. Furthermore, a brittle damage model is used for the reinforcement. Finally, numerical applications are developed by adopting the proposed procedure in order to investigate on the damage of the unreinforced and reinforced masonry panels. © 1998 Elsevier Science Ltd.

1. MOTIVATIONS

The masonry is one of the most used construction material. Nevertheless, the analysis of masonry structures remains one of the most difficult tasks. The difficulty consists mainly in the determination of an effective, i.e. simple and realistic, constitutive law of the masonry material. As a matter of fact, the behavior of the masonry is complex, since it is characterized by nonlinear effects due to the fracture openings and damage of the material.

Because of the low tensile strength of the masonry material, ancient structures often present wide fractures. As a consequence, several kinds of reinforcement have been adopted by structural engineers. The most used materials for the reinforcement of masonry walls are concrete and iron, but nowadays new materials, such as composites, start to be adopted.

Composite materials have been successfully used in several fields of structural engineering, mainly in Aerospace and Mechanical Engineering. Nowadays, fiber-reinforced plastic (FRP) are adopted to replace, or complement, conventional materials also in Civil Engineering (Neale and Labossière, 1992; El-Badry, 1996). In fact, FRP materials exhibit several advantages with respect to traditional ones. They are characterized by low weight and high strength, but also by good resistance to corrosion and durability. Furthermore, although the FRP material is more expansive than many traditional materials, it has reduced installation and maintenance costs.

A review of the applications of advanced composites in Civil Engineering has been proposed by Barbero *et al.* (1994). Therein, it has been noted that FRP rebars can replace the classical steel rebars for the reinforcement of concrete beams, while structural shapes, i.e. FRP composites with prismatic sections, can be used as structural beams.

The composite materials can also be used for repairing old or historical structures. As an example, FRP rebars are used as tendons for prestressing and strengthening concrete and wood structures (Machida, 1993; Nanni, 1993). Meier (1987) proposed the use of prestressed or nonprestressed composite laminates bonded to the external surface of concrete beams for the reinforcement of bridges.

In the last few years, a challenging field of application of FRP in Civil Engineering is the restoring of ancient buildings or monumental structures. Studies of the strengthening of historical masonry structures with advanced composites have been proposed [see e.g.

Triantafillou and Fardis (1993); Schwegler (1994); Triantafillou and Fardis (1995); Triantafillou (1996)]. Two different kinds of reinforcements for the strengthening of masonry structures have been proposed in the literature: by external prestressed rebars, and by bonded composite laminates. Although, sometimes the wrapping of masonry panels by FRP laminas can appear as a blameworthy procedure, it is very effective and can be necessary in critical situations. The behavior of walls, reinforced by carbon fiber sheets or conventional woven fabric bonded on the masonry surfaces, is investigated with experimental tests by Schwegler (1994). A first approach to the modeling of masonry panels reinforced by FRP sheets has been presented by Luciano and Sacco (1996).

In the present work, the mechanical behavior of a masonry wall, unreinforced or reinforced by sheets of FRP composites, is studied. The masonry material is regarded as a composite realized by a regular inclusion of blocks into a matrix of mortar. Hence, the reinforced material obtained by bonding the sheets of composite onto the two surfaces of the masonry is a composite made of composite materials. The overall properties of the unreinforced and reinforced masonry are obtained by applying the homogenization theory.

Herein, a homogenization technique which accounts for the actual geometry of the masonry and for the progressive damage of the mortar, of the block and of the FRP sheets is proposed. In particular, isotropic viscoelastic and elastic damage models, in conjunction with two different strength criteria for the mortar and the block, are proposed, while a two parameters brittle damage model (Jones, 1975) is used for the FRP sheets.

Numerical applications are developed to study the behavior of the unreinforced masonry. Furthermore, the effects of the reinforcement on the response of a masonry panel are investigated. The results emphasize the very special behavior of the reinforced masonry during the damage. In particular, it is emphasized that significative information on the damage of the reinforced masonry can be carried out only by using a micromechanical approach.

2. MICROMECHANICS OF REINFORCED MASONRY

The masonry is a periodic composite material obtained by blocks embedded in a matrix of mortar. In order to determine the overall properties of the composite material, the homogenization theory can be employed (Mura, 1987).

In recent literature, several micromechanical methods have been developed to determine the behavior of the masonry. In particular, in order to evaluate the linear elastic response of the unreinforced masonry, Pande *et al.* (1989) and Kralj *et al.* (1991) used the Mori–Tanaka method and the lamination theory in two steps: initially, the Mori–Tanaka method is adopted to define a transition material obtained by neglecting the presence of the horizontal beds of mortar; then, the lamination theory is employed for the full homogenization. Papa (1990) followed a similar procedure to estimate the overall moduli of the undamaged masonry, and employed a phenomenological method to model the damage process. The two steps homogenization procedure (i.e. the Mori–Tanaka method and the lamination theory) have been adopted by Pietruszczak and Niu (1992), and by Gambarotta and Lagomarsino (1994), to study the progressive failure of the structural masonry. A finite element analysis to derive the overall elastic properties of several periodic masonries has been performed by Anthoine (1995). Recently, Luciano and Sacco (1995, 1997a) proposed a brutal micromechanical model, in conjunction with a finite element procedure for periodic materials, to determine the overall damage of the masonry.

Herein, the overall response of a reinforced masonry material characterized by a regular inclusion of blocks into a matrix of mortar is studied. At this aim, the masonry is regarded as a composite material with periodic microstructure. The reinforcement is realized by two sheets perfectly bonded to the surfaces of the wall, so that the continuity of the displacement field across the interfaces masonry-reinforcement is warranted. Indeed, the assumption of the perfect bonding between the masonry and the FRP sheets fails to be completely valid when damage occurs in the masonry. In fact, experimental evidences show the presence of debonding of FRP sheets in the vicinity of the cracks. In the following, this effect is neglected in order to work with a simpler model.

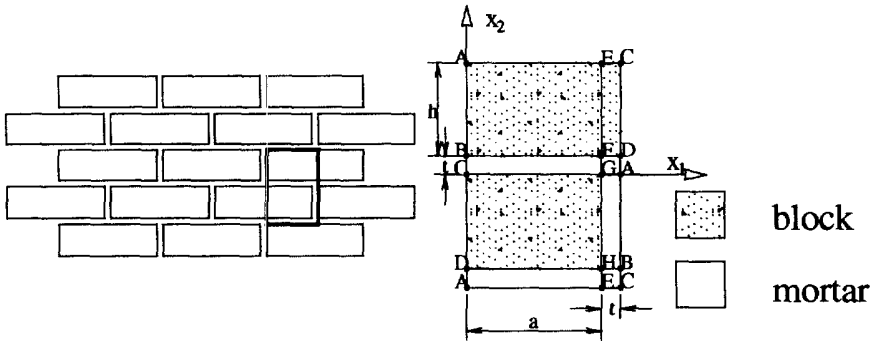

Fig. 1. Schemes of a periodic masonry and of its unit cell.

For a material with periodic microstructure a repetitive unit cell can be determined. In particular, for a regular masonry material, the simple unit cell Ω reported in Fig. 1 is considered. The cell Ω can be decomposed along the thickness direction x_3, in two parts:

$$\Omega^{M} = \{\mathbf{x} \in \Omega : |x_3| \leqslant s^{M}/2\}$$
$$\Omega^{r} = \{\mathbf{x} \in \Omega : s^{M}/2 < |x_3| \leqslant s/2\} \tag{1}$$

where $\Omega^{M} \cup \Omega^{r} = \Omega$, s^{M} is the thickness of the masonry, i.e. the mortar or the block, s^{r} is thickness of laminate of reinforcement and $s = s^{M} + 2s^{r}$ is the thickness of the reinforced masonry. Note that each laminate used as reinforcement consists of N orthotropic layers, with material axes arbitrarily oriented in the plane of the wall. In eqn (1), as well as in the following, the superscripts ^{M}, ^{r}, ^{m} and ^{b} refer to quantities to the masonry, to the reinforcement, to the mortar and to the block, respectively.

Because of the periodicity of the microstructure, the displacement field $\mathbf{u}(\mathbf{x})$ can be represented as (Luciano and Sacco, 1997a, 1997b):

$$\mathbf{u}(\mathbf{x}) = \boldsymbol{\varepsilon}^{0}\mathbf{x} + \mathbf{u}^{p}(\mathbf{x}) \tag{2}$$

where $\mathbf{u}^{p}$ is the part of the displacement periodic in R^2, i.e. in the plane of the wall, and $\boldsymbol{\varepsilon}^{0}$ is an assigned symmetric tensor, with $\varepsilon^{0}_{13} = \varepsilon^{0}_{23} = \varepsilon^{0}_{33} = 0$. For the unit cell Ω reported in Fig. 1, the periodicity condition on $\mathbf{u}^{p}$ requires:

$$\mathbf{u}^{p}(0, x_2, x_3) = \mathbf{u}^{p}(d, x_2 - b, x_3) \qquad \begin{matrix} 0 \leqslant x_2 \leqslant b \\ -s/2 \leqslant x_3 \leqslant s/2 \end{matrix}$$
$$\mathbf{u}^{p}(0, x_2 - b, x_3) = \mathbf{u}^{p}(d, x_2, x_3) \qquad \begin{matrix} 0 \leqslant x_2 \leqslant b \\ -s/2 \leqslant x_3 \leqslant s/2 \end{matrix} \tag{3}$$

$$\mathbf{u}^{p}(x_1, -b, x_3) = \mathbf{u}^{p}(x_1, b, x_3) \qquad \begin{matrix} 0 \leqslant x_1 \leqslant d \\ -s/2 \leqslant x_3 \leqslant s/2 \end{matrix} \tag{4}$$

where $d = a + t$ and $b = h + t$. The special periodicity conditions (3) and (4) are emphasized in Fig. 1, where different points of the boundary of the unit cell, having the same displacement, are denoted by the same identification capital letter. It is worth noting that the strain tensor $\boldsymbol{\varepsilon}^{p}$ associated to the displacement $\mathbf{u}^{p}$ has components ε^{p}_{11}, ε^{p}_{22} and ε^{p}_{12} with null average (Luciano and Sacco, 1997b). Thus, from relation (2) it results in:

$$\bar{\varepsilon}_{\alpha\beta} = \frac{1}{2V}\int_{\Omega}(u_{\alpha,\beta}+u_{\beta,\alpha})\,\mathrm{d}V = \varepsilon^0_{\alpha\beta} \tag{5}$$

where V is the volume of the unit cell Ω. In eqn (5), as well as in the following ones, Greek indices assume values 1 and 2, while Latin indices range from 1 to 3. Note that, because of relation (5), the assigned $\varepsilon^0_{\alpha\beta}$ represents the average of the components $\varepsilon_{\alpha\beta}$ of the strain tensor associated to the displacement field (2).

Further boundary conditions have to be specified on the lateral surfaces of the unit cell Ω, i.e. at $x_3 = \pm s/2$. Since the panel is subjected only to in-plane load, then the tractions on the lateral surfaces of the wall have to be zero:

$$\sigma_{i3}(x_1, x_2, \pm s/2) = 0 \quad \begin{matrix} 0 \leqslant x_1 \leqslant d \\ -b \leqslant x_2 \leqslant b \end{matrix}. \tag{6}$$

Note that the overall behavior of the masonry wall depends on the boundary conditions (6). Different boundary conditions can be considered, provided that their periodicity is preserved.

Isotropic damage models, characterized by evolution laws specified in Section 4, are adopted both for the mortar and the block. The parameter governing the damage of the materials is denoted by β^{mb} and must satisfy the requirement:

$$0 \leqslant \beta^{\mathrm{mb}} \leqslant 1 \quad \text{with} \quad \begin{matrix} \beta^{\mathrm{mb}} = 1 & \text{undamaged material} \\ \beta^{\mathrm{mb}} = 0 & \text{damaged material} \end{matrix} \tag{7}$$

where the superscript $^{\mathrm{mb}}$ stands for $^{\mathrm{m}}$ when it is referred to the mortar, and for $^{\mathrm{b}}$ when it is referred to the block. Note that the quantity β^{mb} is related to the classical damage variable D^{mb} of the continuum damage mechanics (Lemaitre and Chaboche, 1990), by the relation: $\beta^{\mathrm{mb}} = 1 - \mathrm{D}^{\mathrm{mb}}$. Furthermore, a orthotropic damage model, specified in Section 4, is adopted for the FRP sheets. The model considers the longitudinal and the transversal damage parameters χ_{L} and χ_{T} for each layer of the reinforcement, so that the actual constitutive matrix $\tilde{\mathscr{C}}^{\mathrm{r}}$ of the FRP laminate depends on the initial elastic matrix $\mathscr{C}^{\mathrm{r}}$ and on $2N$ parameters $\chi_{\mathrm{L}}^{(1)}, \chi_{\mathrm{T}}^{(1)}, \ldots, \chi_{\mathrm{L}}^{(N)}, \chi_{\mathrm{T}}^{(N)}$.

The instantaneous overall behavior of the masonry is obtained by evaluating the average stress tensor $\boldsymbol{\sigma}^0$ corresponding to the assigned average strain tensor $\boldsymbol{\varepsilon}^0$ applied to the unit cell, with a fixed distribution of the damage parameter β^{mb}. The stress tensor $\boldsymbol{\sigma}^0$ is obtained by averaging the local stress distribution $\boldsymbol{\sigma}$ solution of the following elastostatic problem:

$$\begin{aligned} &\operatorname{div}\boldsymbol{\sigma} = \mathbf{0} \quad \text{in}\,\Omega \\ &\boldsymbol{\varepsilon}^{\mathrm{p}} = \hat{\nabla}\mathbf{u}^{\mathrm{p}} \quad \text{in}\,\Omega \\ &\boldsymbol{\sigma} = \beta^{\mathrm{m}}\mathscr{C}^{\mathrm{m}}(\boldsymbol{\varepsilon}^0 + \boldsymbol{\varepsilon}^{\mathrm{p}}) \quad \text{in}\,\Omega^{\mathrm{m}} \\ &\boldsymbol{\sigma} = \beta^{\mathrm{b}}\mathscr{C}^{\mathrm{b}}(\boldsymbol{\varepsilon}^0 + \boldsymbol{\varepsilon}^{\mathrm{p}}) \quad \text{in}\,\Omega^{\mathrm{b}} \\ &\boldsymbol{\sigma} = \tilde{\mathscr{C}}^{\mathrm{r}}(\boldsymbol{\varepsilon}^0 + \boldsymbol{\varepsilon}^{\mathrm{p}}) \quad \text{in}\,\Omega^{\mathrm{r}} \end{aligned} \tag{8}$$

satisfying the boundary conditions (3), (4) and (6). The symbol $\hat{\nabla}$ stands for the symmetric part of the gradient, $\mathscr{C}^{\mathrm{m}}$ and $\mathscr{C}^{\mathrm{b}}$ are the fourth-order isotropic elastic tensors of the mortar and the block, respectively, and $\tilde{\mathscr{C}}^{\mathrm{r}}$ represents the actual constitutive tensor of the reinforcement material. Once the local distribution of the stress tensor $\boldsymbol{\sigma}$ is determined, the average stress tensor is:

$$\boldsymbol{\sigma}^0 = \frac{1}{V}\int_\Omega \boldsymbol{\sigma}\,\mathrm{d}V.$$

It can be proved that $\sigma_{i3} = 0$. The in-plane components of the average stress tensor, i.e. $\sigma^0_{\alpha\beta}$, associated to a given in-plane average strain tensor with components $\varepsilon^0_{\gamma\delta} = \varepsilon^0_{\delta\gamma} = 1$ and $\varepsilon^0_{\lambda\mu} = \varepsilon^0_{\mu\lambda} = 0$ for $\lambda, \mu \neq \gamma, \delta$, represent the in-plane elastic moduli $\bar{\mathscr{C}}_{\alpha\beta\gamma\delta}$ of the homogenized reinforced masonry panel. It is worth noting that the proposed procedure allows to determine the in-plane overall properties of the masonry wall, by performing a three-dimensional analysis, i.e. by completely accounting for the strain and stress in the direction transversal to the panel.

The elastostatic problem (8) with the constraints (3)–(6) can be approached by adopting one of the variational formulations proposed by Luciano and Sacco (1996b). In particular, herein the solution of the elastostatic problem is computed by minimizing the total potential energy:

$$\pi(\mathbf{u}^{\mathrm{p}}) = \frac{1}{2}\int_{\Omega^{\mathrm{M}}} \beta^{\mathrm{mb}}\mathscr{C}^{\mathrm{mb}}[\boldsymbol{\varepsilon}^0 + \hat{\nabla}\mathbf{u}^{\mathrm{p}}]\cdot(\boldsymbol{\varepsilon}^0 + \hat{\nabla}\mathbf{u}^{\mathrm{p}})\,\mathrm{d}V + \frac{1}{2}\int_{\Omega^{\mathrm{r}}} \tilde{\mathscr{C}}^{\mathrm{r}}[\boldsymbol{\varepsilon}^0 + \hat{\nabla}\mathbf{u}^{\mathrm{p}}]\cdot(\boldsymbol{\varepsilon}^0 + \hat{\nabla}\mathbf{u}^{\mathrm{p}})\,\mathrm{d}V. \quad (9)$$

3. HOMOGENIZATION PROCEDURE

A simplified approach to minimize the functional (9), which leads to a homogenization procedure, is proposed. As shown in Fig. 1, the cell is decomposed in eight subcells. Each subcell, with in-plane dimensions L_1 and L_2, is a finite element where the displacements u^{p}_1 and u^{p}_2 are approximated by bilinear interpolation functions of local coordinate x'_1 and x'_2, with origin in the center of the subcell, and by a constant function in the thickness direction. Furthermore, in the whole cell Ω, the transversal displacement u^{p}_3 is assumed to be a constant function of x_1 and x_2, and a linear function of x_3. Hence, for the typical ith subcell defined by the nodes $I-J-H-K$, it is assumed:

$$u^{\mathrm{p}}_\alpha(x'_1, x'_2, x_3) = u^{\mathrm{p(I)}}_\alpha \frac{1}{4}\left(1-\frac{2x'_1}{L_1}\right)\left(1-\frac{2x'_2}{L_2}\right) + u^{\mathrm{p(J)}}_\alpha \frac{1}{4}\left(1+\frac{2x'_1}{L_1}\right)\left(1-\frac{2x'_2}{L_2}\right)$$
$$+ u^{\mathrm{p(H)}}_\alpha \frac{1}{4}\left(1+\frac{2x'_1}{L_1}\right)\left(1+\frac{2x'_2}{L_2}\right) + u^{\mathrm{p(K)}}_\alpha \frac{1}{4}\left(1-\frac{2x'_1}{L_1}\right)\left(1+\frac{2x'_2}{L_2}\right) \quad (10)$$

$$u^{\mathrm{p}}_3(x_1, x_2, x_3) = x_3 w. \quad (11)$$

It can be noted that the strain corresponding to the displacement (10) and (11) has components $\varepsilon^{\mathrm{p}}_{13} = \varepsilon^{\mathrm{p}}_{23} = 0$. Hence, the transversal shear deformation of the wall is neglected. Since $\varepsilon^0_{13} = \varepsilon^0_{23} = 0$, the total shear deformation in the thickness of the panel is zero, in fact $\varepsilon^0_{13} + \varepsilon^{\mathrm{p}}_{13} = 0$ and $\varepsilon^0_{23} + \varepsilon^{\mathrm{p}}_{23} = 0$. Thus, for $\mathscr{C}^{\mathrm{mb}}$ and $\tilde{\mathscr{C}}^{\mathrm{r}}$ isotropic and orthotropic elastic tensors, respectively, the transversal shear stresses are zeros, i.e. $\sigma_{23} = \sigma_{13} = 0$.

For a simpler notation, let $\boldsymbol{\tau} = \{\sigma_{11}, \sigma_{22}, \sigma_{12}, \sigma_{33}\}$ denote the vector of the non-trivial ordered stress components, and let $\mathbf{e} = \{\varepsilon_{11}, \varepsilon_{22}, 2\varepsilon_{12}, \varepsilon_{33}\}$ be the vector of the non-trivial ordered strain components. The constitutive relationships for the mortar and the block becomes:

$$\boldsymbol{\tau}^{\mathrm{mb}} = \beta^{\mathrm{mb}}\mathbf{C}^{\mathrm{mb}}(\mathbf{e}^0 + \mathbf{e}^{\mathrm{p}}) \quad \text{in} \quad \Omega^{\mathrm{mb}} \quad (12)$$

where $\mathbf{C}^{\mathrm{mb}}$ represents the reduced elastic matrix. As concerns the reinforcement, the stress–strain relationship in the (x_1, x_2, x_3)-coordinate is:

$$\tau^r = \tilde{\mathbf{C}}^r(\mathbf{e}^0 + \mathbf{e}^p) \quad \text{in} \quad \Omega^r \tag{13}$$

where $\tilde{\mathbf{C}}^r$ is the reduced actual matrix of the laminate in the global coordinate system.

By substituting the expressions (10) and (11) in the total potential energy (9), and taking into account eqns (12) and (13), with the damage parameter β^{mb} constant in each subcell, the stationary condition for the total potential energy leads to:

$$(\beta^{mb(i)}\mathbf{K}^{mb(i)} + \mathbf{K}^{r(i)})\mathbf{U}^{(i)} - \mathbf{E}^{(i)} = \mathbf{0}. \tag{14}$$

The vector of the nodal displacements of the ith subcell is:

$$\mathbf{U}^{(i)} = \{u_1^{p(I)} \quad u_2^{p(I)} \quad u_1^{p(J)} \quad u_2^{p(J)} \quad u_1^{p(H)} \quad u_2^{p(H)} \quad u_1^{p(K)} \quad u_2^{p(K)} \quad w\}.$$

The symmetric stiffness matrices $\mathbf{K}^{mb(i)}$ and $\mathbf{K}^{r(i)}$ can be written as:

$$\mathbf{K}^{(i)} = \begin{bmatrix} k_1/3 & k_2 & k_3 & k_4 & -k_1/6 & -k_2 & k_5 & -k_4 & k_6 \\ & k_7/3 & -k_4 & k_8 & -k_2 & -k_7/6 & k_4 & k_9 & k_{10} \\ & & k_1/3 & -k_2 & k_5 & k_4 & -k_9/6 & k_2 & -k_6 \\ & & & k_7/3 & -k_4 & k_9 & k_2 & -k_7/6 & k_{10} \\ & & & & k_1/3 & k_2 & k_3 & k_4 & -k_6 \\ & & & & & k_7/3 & -k_4 & k_8 & -k_{10} \\ & & & & & & k_1/3 & -k_2 & k_6 \\ & & & & & & & k_7/3 & -k_{10} \\ & & & & & & & & C_{44}L_1L_2 \end{bmatrix}$$

with

$$k_1 = \frac{C_{33}L_1^2 + C_{11}L_2^2}{L_1L_2} \quad k_2 = \frac{C_{12} + C_{33}}{4} \quad k_3 = \frac{C_{33}L_1^2 - 2C_{11}L_2^2}{6L_1L_2}$$

$$k_4 = \frac{C_{12} - C_{33}}{4} \quad k_5 = \frac{C_{11}L_2^2 - 2C_{33}L_1^2}{6L_1L_2} \quad k_6 = -\frac{L_2C_{14}}{2}$$

$$k_7 = \frac{C_{22}L_1^2 + C_{33}L_2^2}{L_1L_2} \quad k_8 = \frac{C_{22}L_1^2 - 2C_{33}L_2^2}{6L_1L_2} \quad k_9 = \frac{C_{33}L_2^2 - 2C_{22}L_1^2}{6L_1L_2}$$

$$k_{10} = -\frac{C_{24}L_1}{2}.$$

Further, the vector of the known terms is:

$$E_1^{(i)} = -\frac{C_{33}e_3^0L_1 + C_{12}e_2^0L_2 + C_{11}e_1^0L_2}{2}$$

$$E_2^{(i)} = -\frac{C_{22}e_2^0L_1 + C_{33}e_3^0L_2 + C_{12}e_1^0L_1}{2}$$

$$E_3^{(i)} = -\frac{C_{33}e_3^0L_1 - C_{12}e_2^0L_2 - C_{11}e_1^0L_2}{2}$$

$$E_4^{(i)} = \frac{C_{33}e_3^0 L_2 - C_{22}e_2^0 L_1 - C_{12}e_1^0 L_1}{2}$$

$$E_5^{(i)} = -E_1^{(i)} \quad E_6^{(i)} = -E_2^{(i)}$$

$$E_7^{(i)} = -E_3^{(i)} \quad E_8^{(i)} = -E_4^{(i)}$$

$$E_9^{(i)} = L_1 L_2 (C_{14}e_1^0 + C_{24}e_2^0).$$

Note that $\mathbf{C} = \mathbf{C}^{mb}$ for the mortar or the block and $\mathbf{C} = \tilde{\mathbf{C}}^{r}$ for the reinforcement.

Finally, by denoting with $\mathbf{U}$ the global displacement vector and with $\mathbf{Q}^{(i)}$ the matrices such that:

$$\mathbf{U} = \sum_{i=1}^{8} \mathbf{Q}^{(i)}\mathbf{U}^{(i)}$$

the global stiffness matrix of the unit cell $\mathbf{K}$ can be written as

$$\mathbf{K} = \sum_{i=1}^{8} \hat{\mathbf{K}}^{r(i)} + \gamma_a \hat{\mathbf{K}}^{b(1)} + \gamma_b \hat{\mathbf{K}}^{b(2)} + \gamma_c \hat{\mathbf{K}}^{b(5)} + \beta_a(\hat{\mathbf{K}}^{m(3)} + \hat{\mathbf{K}}^{m(4)}) + \beta_b(\hat{\mathbf{K}}^{m(7)} + \hat{\mathbf{K}}^{m(8)}) + \beta_c \hat{\mathbf{K}}^{m(6)}$$

where

$$\hat{\mathbf{K}}^{(i)} = \mathbf{Q}^{(i)^T}\mathbf{K}^{(i)}\mathbf{Q}^{(i)}, \gamma_a = \beta^{b(1)}, \gamma_b = \beta^{b(2)}, \gamma_c = \beta^{b(5)}, \beta_a = \beta^{m(3)} = \beta^{m(4)}, \beta_b = \beta^{m(7)} = \beta^{m(8)}$$

and $\beta_c = \beta^{b(6)}$.

The global vector of the known terms is:

$$\mathbf{E} = \sum_{i=1}^{8} \mathbf{Q}^{(i)}\mathbf{E}^{(i)}.$$

Hence, the approximated form of the periodic elastostatic problem of the unit cell is governed by the equation:

$$\mathbf{KU} - \mathbf{E} = \mathbf{0}. \tag{15}$$

By assigning the strain $\mathbf{e}^0$, with e_1^0, e_2^0 and e_3^0 representing the average of the strain components, the nodal displacement vector $\mathbf{U}$ is determined by solving the algebraic eqn (15). Then, the strain and the stress distributions can be computed. Hence, it is possible to evaluate the average stresses in the reinforced masonry, i.e. τ^0, in the masonry, i.e. τ^M, and in the reinforcement, i.e. τ^r. Furthermore, when the strain $\mathbf{e}^0 = \{1, 0, 0, 0\}$ is assigned, the average of the first three components of the stress τ^0 gives the first column of the effective instantaneous elastic moduli $\bar{\mathbf{C}}$ of the reinforced panel. Analogously, when it is taken $\mathbf{e}^0 = \{0, 1, 0, 0\}$ and $\mathbf{e}^0 = \{0, 0, 1, 0\}$, the average stresses τ_i^0 with $i = 1, 2, 3$ give the second and the third columns of $\bar{\mathbf{C}}$, respectively. In such a way, the in-plane elastic moduli of the reinforced masonry wall, which accounts for the transversal effects, are obtained. It can be recalled that the average of the fourth component of the strain $\mathbf{e}$, i.e. the mean transversal strain $\bar{e}_4$, could be not zero, because of the presence of the boundary condition (6).

4. DAMAGE EVOLUTION LAWS

The constituents of the reinforced masonry material have different constitutive laws. Next, two isotropic damage models are proposed for the mortar and the block : a viscoelastic

and an elastic damage law. Furthermore, a brittle damage model is adopted for the FRP sheets.

4.1. *Viscoelastic damage model for block and mortar*

The viscoelastic isotropic damage model developed by Frémond and Nedjar (1996a, 1996b) can be adopted for the mortar and the block. Thus, the constitutive equations in eqn (8) can be completed by the evolution law for the damage parameter. To this end, it is set:

$$\dot{\beta}^{mb} = \frac{\langle \varphi^{mb} \rangle}{c^{mb}} \left[M^{mb} \frac{1-\beta^{mb}}{\beta^{mb}|\varphi^{mb}|} - 1 \right] \leqslant 0 \tag{16}$$

with

$$\varphi^{mb} = \psi^{mb}(\mathbf{e}) - \omega^{mb} \tag{17}$$

where c^{mb} is the viscosity parameter, ω^{mb} is the damage threshold energy per unit of volume, ψ^{mb} is the energy of damage per unit of volume, M^{mb} is the factor of displacement of ω^{mb}, and $\langle \cdot \rangle$ is the Macaulay bracket which selects the positive part of a number. The quantities c^{mb}, ω^{mb} and M^{mb} are material parameters, and assume different values for the mortar and the block. The energy ψ^{mb} is a function of the deformation state, and has different expressions for the mortar and the block. Note that φ^{mb} represents the so-called yield function in the strain space.

Experimental evidences for one-dimensional specimen often show different damage behaviors in compression and in tension tests. As a consequence, different values for the damage parameters c^{mb} and M^{mb} can be chosen for the two cases. Next, in the framework of isotropic damage, it is assumed that for multi-dimensional strain states, the sign of trace of strain tensor $\eta = e_1 + e_2 + e_4$ detects the compression or the tension case. Thus, when $\eta > 0$ it is set $c^{mb} = c^{mb(+)}$ and $M^{mb} = M^{mb(+)}$, when $\eta < 0$ it is set $c^{mb} = c^{mb(-)}$ and $M^{mb} = M^{mb(-)}$.

4.2. *Elastic damage model for block and mortar*

An elastic isotropic damage model for the mortar and the block is proposed. In particular, the following evolution law for the damage parameter is considered:

$$\dot{\beta}^{mb} = c_2 k^{mb} \exp(-f^2)[\exp(k^{mb}\langle \varphi^{mb} \rangle) - 2f(\exp(f) - 1)]\overline{\langle \varphi^{mb} \rangle} \leqslant 0 \tag{18}$$

where $f = c_1 + k^{mb}\langle \varphi^{mb} \rangle$. Contrarily to the viscoelastic case (16), the evolution law (18) can be integrated in closed form with respect to time. Thus, for a monotonic loading path, the damage is:

$$\beta^{mb} = c_2 \exp(-f^2)(\exp(f) - 1). \tag{19}$$

The constants c_1 and c_2 are set such that $\beta^{mb} = 1$ for $\varphi^{mb} = 0$ and $\beta^{mb} \to 0$ for $\varphi^{mb} \to +\infty$; in particular, it is taken that $c_1 = 0.864162$ and $c_2 = 1.536897$. The quantity k^{mb} is a material parameter which controls the softening part of the stress–strain relationship. By increasing the value of k^{mb} a more and more brittle behavior of the material is obtained.

As proposed for the previous viscoelastic damage law, also for the present elastic damage model different values for the damage parameter k^{mb} can be chosen for the case of tension or compression. Hence, for $\eta > 0$ it is set $k^{mb} = k^{mb(+)}$, for $\eta < 0$ it is set $k^{mb} = k^{mb(-)}$.

4.3. *Energy of damage*

The mortar plays the role of joints in the pattern of the masonry. Thus, the damage of these joints is mainly governed by the normal and tangential strains. Hence, it can be supposed that the strain in the joint direction does not affect the strength of a mortar joint.

Let e_n and e_3 denote the normal and shear strains in a typical joint, with $e_n = e_1$ for the vertical joints and $e_n = e_2$ for the horizontal joints; the energy ψ^m is assumed to have the form:

$$\psi^m(e_n, e_3) = \tfrac{1}{2}[C^m_{nn}(\langle e_n\rangle^2 + \alpha\langle -e_n\rangle^2) + C^m_{33}e_3^2] \tag{20}$$

where α is a coefficient less than 1, which allows to account for a different strength in traction and in compression. It can be noted that, according to expression (20), the transversal strain e_4 is not responsible for the damage of the mortar joint. Because of the isotropy of the mortar material, the energy of damage ψ^m assumes the form:

$$\psi^m(e_n, e_3) = \frac{E^m}{4(1+\nu^m)}\left[\frac{2(1-\nu^m)}{(1-2\nu^m)}(\langle e_n\rangle^2 + \alpha\langle -e_n\rangle^2) + e_3^2\right] \tag{21}$$

where E^m and ν^m are the Young's modulus and the Poisson's ratio. In order to determine the mechanical meaning of the parameter α, let $\sigma^c > 0$ and $\sigma^t > 0$ denote the limit strengths in compression and in traction of the mortar material, respectively, obtained by uniaxial tests. When a limit strength is attained, then $\varphi^m = 0$ and hence eqn (17) with eqn (21) gives, for the compression and for the tension case:

$$\omega^m \frac{E^m}{(\sigma^c)^2} = \frac{1}{4(1+\nu^m)}\left[\frac{2(1-\nu^m)}{(1-2\nu^m)}\alpha\right] \tag{22}$$

$$\omega^m \frac{E^m}{(\sigma^t)^2} = \frac{1}{4(1+\nu^m)}\left[\frac{2(1-\nu^m)}{(1-2\nu^m)}\right] \tag{23}$$

respectively. Equations (22) and (23) allow to determine the relation:

$$\sigma^t = \sqrt{\alpha}\sigma^c.$$

Furthermore, by taking into account the eqn (22), the yield function can assume the equivalent form:

$$\varphi^m \frac{E^m}{(\sigma^c)^2} = \frac{1}{4(1+\nu^m)}\left[\frac{2(1-\nu^m)}{(1-2\nu^m)}\left(\left\langle \frac{e_n E^m}{\sigma^c}\right\rangle^2 + \alpha\left\langle -\frac{e_n E^m}{\sigma^c}\right\rangle^2 - \alpha\right) + \left(\frac{e_3 E^m}{\sigma^c}\right)^2\right]. \tag{24}$$

The limit contours of the proposed yield function (24) computed for several values of Poisson ratio ν^m, when $\alpha = 0.04$, are reported in Fig. 2 in the space $e_n E^m/\sigma^c$, $e_3 E^m/\sigma^c$.

As concerns the block, a generalization of a strength criterion proposed for the concrete by Mazars (1984) and Mazars and Pijaudier-Cabot (1989), and reported also in (Lemaitre and Chaboche, 1990), is adopted. In particular, it is set:

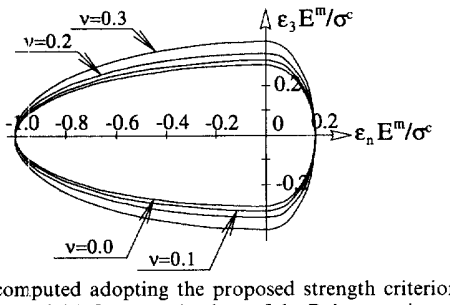

Fig. 2. Limit contours computed adopting the proposed strength criterion for the mortar when $\alpha = 0.04$, for several values of the Poisson ratio.

$$\psi^{b}(\mathbf{e}) = \tfrac{1}{2}(L_{11}\langle\varepsilon_1\rangle^2 + L_{22}\langle\varepsilon_2\rangle^2 + L_{44}\langle e_4\rangle^2) + L_{12}\langle\varepsilon_1\rangle\langle\varepsilon_2\rangle + L_{14}\langle\varepsilon_1\rangle\langle e_4\rangle + L_{24}\langle\varepsilon_2\rangle\langle e_4\rangle \tag{25}$$

where ε_1 and ε_2 are principal strains. When it is assumed $L_{ii} = 2$, with $i = 1, 2, 4$ and $L_{ij} = 0$, with $i \neq j$, the Mazars energy of fracture is obtained:

$$\tilde{\psi}^{b}(\mathbf{e}) = \langle\varepsilon_1\rangle^2 + \langle\varepsilon_2\rangle^2 + \langle e_4\rangle^2. \tag{26}$$

In the following, it is proposed the case $L_{ij} = C^{b}_{ij}$, hence the energy of fracture takes the form:

$$\hat{\psi}^{b}(\mathbf{e}) = \frac{E^{b}}{2(1+\nu^{b})(1-2\nu^{b})}[(1-\nu^{b})(\langle\varepsilon_1\rangle^2 + \langle\varepsilon_2\rangle^2 + \langle e_4\rangle^2) + 2\nu^{b}(\langle\varepsilon_1\rangle\langle\varepsilon_2\rangle + \langle\varepsilon_1\rangle\langle e_4\rangle + \langle\varepsilon_2\rangle\langle e_4\rangle)]. \tag{27}$$

It can be emphasized that, when a limit strength in compression σ^{c} is given, then the limit strength in tension σ^{t} is uniquely determined as a function of σ^{c}. Next, the difference between the limit tensile strengths obtained by the Mazars and by the proposed damage criteria, for a given σ^{c}, is determined. The principal strains corresponding to the uniaxial limit strength in compression $\sigma^{c} > 0$ are:

$$\varepsilon_1 = -\frac{\sigma^{c}}{E^{b}} < 0, \quad \varepsilon_2 = e_4 = \nu^{b}\frac{\sigma^{c}}{E^{b}} > 0.$$

Hence, the limit damage energy for the Mazars (26) and the proposed (27) criteria assumes the value:

$$\tilde{\omega}^{b} = \tilde{\psi}^{b}(\mathbf{e}) = 2\left(\frac{\nu^{b}\sigma^{c}}{E^{b}}\right)^2 \tag{28}$$

$$\hat{\omega}^{b} = \hat{\psi}^{b}(\mathbf{e}) = \frac{(\nu^{b}\sigma^{c})^2}{(1+\nu^{b})(1-2\nu^{b})E^{b}} \tag{29}$$

respectively. On the other hand, the principal strains associated to the limit tensile stress σ^{t} are:

$$\varepsilon_1 = \frac{\sigma^{t}}{E^{b}} > 0, \quad \varepsilon_2 = e_4 = -\nu^{m}\frac{\sigma^{t}}{E^{b}} < 0.$$

Thus, when the limit strength in traction is attained, for the Mazars and the proposed criteria it occurs:

$$\tilde{\omega}^{b} = \tilde{\psi}^{b}(\mathbf{e}) = \left(\frac{\tilde{\sigma}^{t}}{E^{b}}\right)^2 \tag{30}$$

$$\hat{\omega}^{b} = \hat{\psi}^{b}(\mathbf{e}) = \frac{(1-\nu^{b})(\hat{\sigma}^{t})^2}{2(1+\nu^{b})(1-2\nu^{b})E^{b}}. \tag{31}$$

A simple comparison of the formulas (28) and (29) with (30) and (31), respectively, reveals

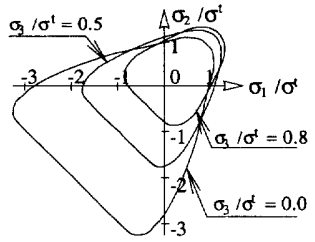

Fig. 3. Limit contours computed adopting the proposed strength criterion for the block, for several values of the limit tension.

that, according to the Mazars and to the proposed criteria, the limit strengths in traction are:

$$\tilde{\sigma}^t = \sqrt{2}\nu^b\sigma^c, \quad \hat{\sigma}^t = \sqrt{\frac{2}{(1-\nu^b)}}\nu^b\sigma^c \tag{32}$$

respectively. Formula (32) shows that, for a given σ^c, the limit strength $\tilde{\sigma}^t$ is always lower than $\hat{\sigma}^t$.

The limit contours for $\sigma_3/\sigma^t = 0.0$, $\sigma_3/\sigma^t = 0.5$ and $\sigma_3/\sigma^t = 0.8$, computed by using the proposed strength criterion, with $\sigma^t = \hat{\sigma}^t$, are reported in Fig. 3 for the case $\nu = 0.25$.

4.4. *Brittle damage model for FRP sheets*

Next, a very simple orthotropic damage model for the FRP material, based on the Tsai–Hill failure criterion, is considered. Let σ_L, σ_T and σ_{LT} be the longitudinal, the transversal and the shear stresses in the material direction of a composite lamina, the following quantities are introduced:

$$F_L = \left(\frac{\sigma_L}{X}\right)^2 \quad F_T = \left(\frac{\sigma_T}{Y}\right)^2 + \left(\frac{\sigma_{LT}}{S}\right)^2$$

where X and Y are the strengths in the longitudinal and transversal direction, respectively, and S is the shear strength. According to the Tsai–Hill criterion, the failure of a lamina occurs when the following equation is verified:

$$F = F_L - \frac{\sigma_L\sigma_T}{X^2} + F_T = 1. \tag{33}$$

Since advanced composite material show a brittle behavior, it is assumed that when the failure eqn (33) is verified a sudden reduction of stiffness occurs for the material. In particular, the two damage parameters χ_L and χ_T are introduced, such that:

$$0 \leqslant \chi_{L(T)} \leqslant 1 \quad \text{with} \quad \begin{array}{ll} \chi_{L(T)} = 1 & \text{undamaged material in L(T)-direction} \\ \chi_{L(T)} = 0 & \text{damaged material L(T)-direction.} \end{array} \tag{34}$$

Initially, it is set $\chi_L = \chi_T = 1$; the evolution of the damage parameters depends on the value of F and of the ratio F_L/F_T, according to the equations:

$$\begin{aligned} &F = 1 \quad \text{and} \quad F_L/F_T > 1 \Rightarrow \chi_L = 0 \\ &F = 1 \quad \text{and} \quad F_L/F_T \leqslant 1 \Rightarrow \chi_T = 0. \end{aligned} \tag{35}$$

Furthermore, because of the second principle of the thermodynamics, the damage parameters have to satisfy the evolutionary conditions $\dot{\chi}_L \leqslant 0$ and $\dot{\chi}_T \leqslant 0$. Finally, the actual

constitutive matrix, in the material system, of the kth layer of the reinforcement is given as:

$$\tilde{\mathbf{C}}^{r(k)} = \begin{bmatrix} \chi_L C_{11}^{r(k)} & \chi_L \chi_T C_{12}^{r(k)} & 0 \\ \chi_L \chi_T C_{12}^{r(k)} & \chi_T C_{22}^{r(k)} & 0 \\ 0 & 0 & \chi_L \chi_T C_{33}^{r(k)} \end{bmatrix}.$$

5. APPLICATIONS

The behavior of a specific masonry material is studied. The elastic properties of the mortar and block materials are:

$$E^m = 1000 \text{ MPa}, \quad \nu^m = 0.30$$

$$E^b = 15{,}000 \text{ MPa}, \quad \nu^b = 0.25.$$

As concerns the parameters characterizing the viscoelastic damage constitutive law, different values for c^b, M^b, c^m and M^m are considered for the tensile and the compressive case:

$$\omega^m = 0.15e-3 \text{ MPa}, \quad \alpha = 0.04$$

$$M^{m(+)} = 0.10e-4 \text{ MPa}, \quad c^{m(+)} = 0.10e-5 \text{ MPa} \cdot \text{s}$$

$$M^{m(-)} = 0.50e-4 \text{ MPa}, \quad c^{m(-)} = 0.50e-5 \text{ MPa} \cdot \text{s}$$

$$\omega^b = 0.10e-3 \text{ MPa}$$

$$M^{b(+)} = 0.75e-4 \text{ MPa}, \quad c^{b(+)} = 0.50e-6 \text{ MPa} \cdot \text{s}$$

$$M^{b(-)} = 0.50e-3 \text{ MPa}, \quad c^{b(-)} = 0.50e-4 \text{ MPa} \cdot \text{s}.$$

The strain rate is always taken to be $\dot{\varepsilon} = 0.1 \text{ s}^{-1}$. For the elastic damage constitutive law, is considered the following case:

$$k^{m(+)} = 2000 \text{ MPa}^{-1}, \quad k^{b(+)} = 2500 \text{ MPa}^{-1}$$

$$k^{m(-)} = 2500 \text{ MPa}^{-1}, \quad k^{b(-)} = 180 \text{ MPa}^{-1}.$$

In Figs 4 and 5 the uniaxial stress–strain responses in traction and in compression of the mortar and the block materials subjected to viscoelastic and elastic damage are plotted.

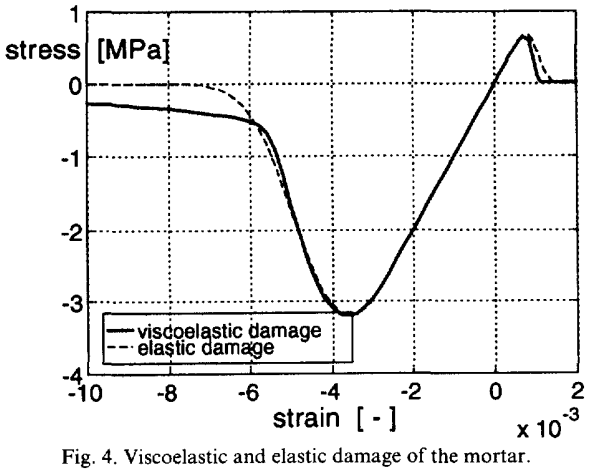

Fig. 4. Viscoelastic and elastic damage of the mortar.

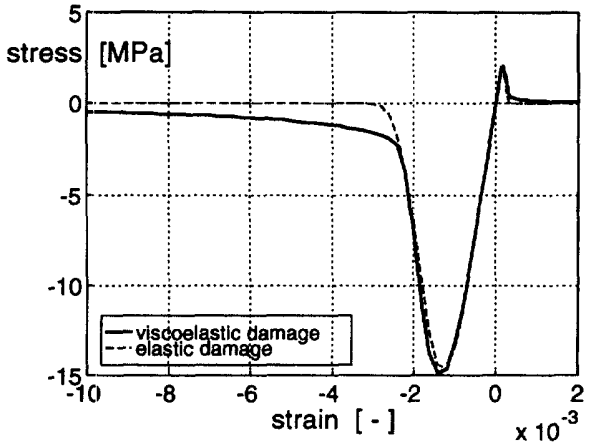

Fig. 5. Viscoelastic and elastic damage of the block.

Figures 4 and 5 show that an opportune choice of the damage parameters for the viscoelastic and the elastic models allows to capture the same behavior of the materials. The micro-structural geometry of the masonry panel is defined by (see Fig. 1):

$$a = 105 \text{ mm}, \quad h = 75 \text{ mm}$$

$$t = 15 \text{ mm}, \quad s^{\mathrm{M}} = 500 \text{ mm}.$$

In the following, computations for the masonry wall are carried out by considering both the elastic and the viscoelastic damage models. In particular, it is assumed for the composite the same strain rate previously adopted for the mortar and the block, i.e. $\dot{\varepsilon} = 0.1$ s^{-1}.

In Figs 6–8 the values of the forces $t_1 = \tau_1^{\mathrm{M}} * s^{\mathrm{M}}$, $t_2 = \tau_2^{\mathrm{M}} * s^{\mathrm{M}}$ and $t_3 = \tau_3^{\mathrm{M}} * s^{\mathrm{M}}$ per unit of length of unreinforced masonry material corresponding to the three assigned average strains $\mathbf{e}^0 = \{e_1, 0, 0, 0\}$, $\mathbf{e}^0 = \{0, e_2, 0, 0\}$ and $\mathbf{e}^0 = \{0, 0, e_3, 0\}$ are plotted, respectively. The different behavior of the masonry material can be noted when the elastic or the viscoelastic damage model proposed is used. Indeed, the mortar is more deformable than the block, hence a concentration of strain in the mortar joints occurs. Furthermore, the mortar and the block are subjected to strain rates higher and lower, respectively, than the one applied on the whole masonry specimen.

Since the elastic damage depends only on the value of the strain, the concentration of deformation in the mortar joints leads to a sudden damage of the mortar, and then to a quite brittle overall behavior of the masonry. On the other hand, the viscoelastic damage

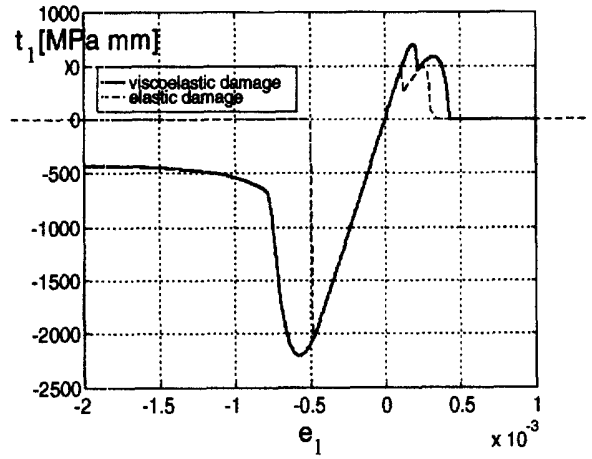

Fig. 6. Average force per unit of length t_1 vs average strain e_1 for unreinforced masonry.

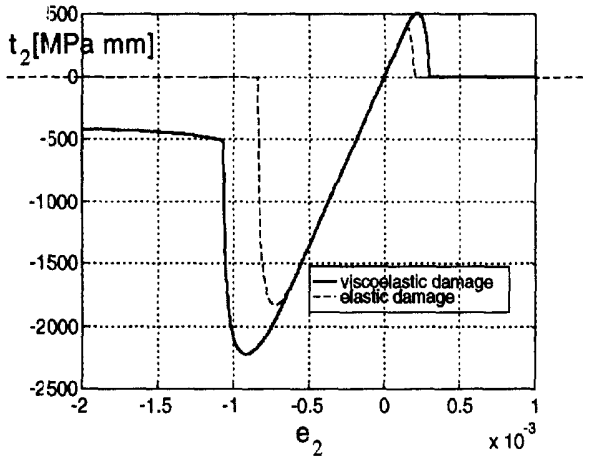

Fig. 7. Average force per unit of length t_2 vs average strain e_2 for unreinforced masonry.

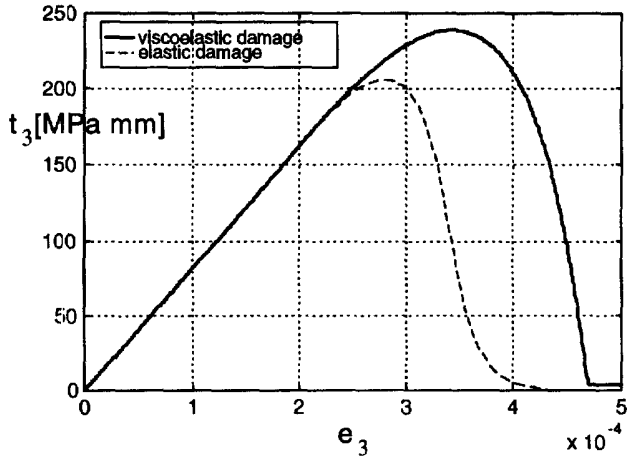

Fig. 8. Average force per unit of length t_3 vs average strain e_3 for unreinforced masonry.

model is governed by the strain, and even by the strain rate. Indeed, the mortar and the block are subjected to strain rates higher and lower, respectively, than the ones adopted in Figs 4 and 5. As a consequence, the mortar and the block in the masonry have strengths higher and lower, respectively, than the ones shown in Figs 4 and 5. Thus, the masonry presents a higher overall limit strength of viscoelastic damage model than for the elastic one. Furthermore, when the masonry is subjected to compressive tests, the damage of the block, due to the transversal strain, strongly influences the overall behavior of the masonry. In fact, as pointed out by Hilsdorf (1969), when a masonry wall is loaded by an in-plane compression, the different deformability of the brick and the mortar induces tensile and compressive transversal stresses in the brick and in the mortar, respectively. Thus, the traction in the thickness of the block could lead to a transversal failure of the wall. Since the damage model proposed in the previous section consider at all the transversal strain and stress in the block, the Hilsdorf effect is completely accounted for. In particular, when the viscoelastic damage model is adopted, the presence of the transversal normal stress τ_4^M in the masonry wall is responsible for a reduction of its in-plane compressive strength.

Next, the case of reinforced masonry is considered. The elastic damage evolution laws for the mortar, the block and the laminate are adopted for the computations. The reinforcement of the masonry wall is made of a two-layer angle-ply $-45°/45°$ graphite–epoxy laminate, with thickness of the single layer $s^r = 1$ mm. The elastic properties of the laminate are:

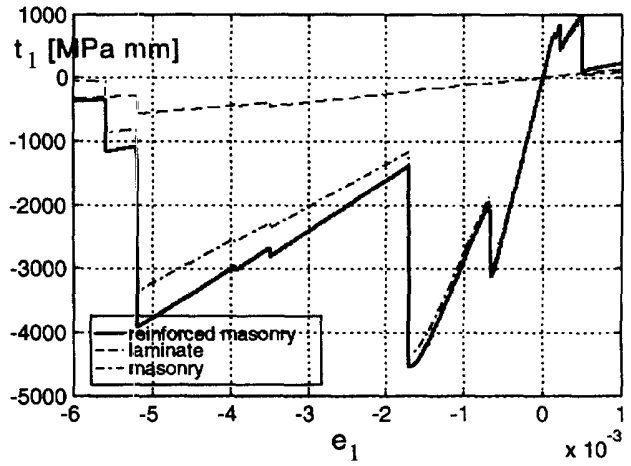

Fig. 9. Average force per unit of length t_1, t_1^M and t_1^r vs average strain e_1 for reinforced masonry.

$$E_L^r = 105{,}000 \text{ MPa}, \quad E_T^r = 7700 \text{ MPa}, \quad G_{LT}^r = 4006 \text{ MPa}$$
$$X = 1000 \text{ MPa}, \quad Y = 50 \text{ MPa}, \quad S = 30 \text{ MPa}$$

with $\nu_{TL}^r = 0.30$.

In Fig. 9 the forces per unit of length $t_1^M = \tau_1^M * s^M$, $t_1^r = 2\tau_1^r * s^r$ and $t_1 = t_1^M + t_1^r$ occurring in the masonry, in the reinforcement and in the reinforced masonry, respectively, corresponding to the assigned average strains $\mathbf{e}^0 = \{e_1, 0, 0, 0\}$ is plotted. Analogously, in Figs 10 and 11 the forces per unit of length t_2^M, t_2^r, t_2 and t_3^M, t_3^r, t_3, corresponding to assigned average strains $\mathbf{e}^0 = \{0, e_2, 0, 0\}$ and $\mathbf{e}^0 = \{0, 0, e_3, 0\}$, respectively, are plotted.

Figures 9–11 reveal the particular and very interesting behavior of the reinforced masonry. It can be noted that for any type of loading condition, the mortar is the first constituent which fails. After the complete degradation of the mortar, a composite realized by blocks connected by the laminate is obtained. Hence, under the increasing loading, the damage of the block or of the laminate can occur. For the particular case investigated, Figs 9–11 show that the block fails before the laminate when the reinforced masonry is subjected to extension or to shear deformation, while the laminate between two adjacent blocks fails before the blocks when it is subjected to compression. This special behavior can be explained by observing that after the degradation of the mortar, the reinforced masonry is a composite highly deformable in the zones where the mortar is damaged. Thus, strain concentrations between adjacent blocks occur, leading to high stretches of the laminate. On the other hand, the blocks can support reduced tensile stresses, but they have a quite high strength in

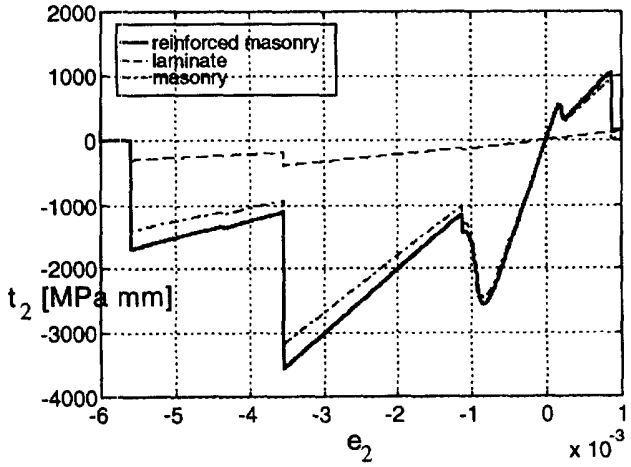

Fig. 10. Average force per unit of length t_2, t_2^M and t_2^r vs average strain e_2 for reinforced masonry.

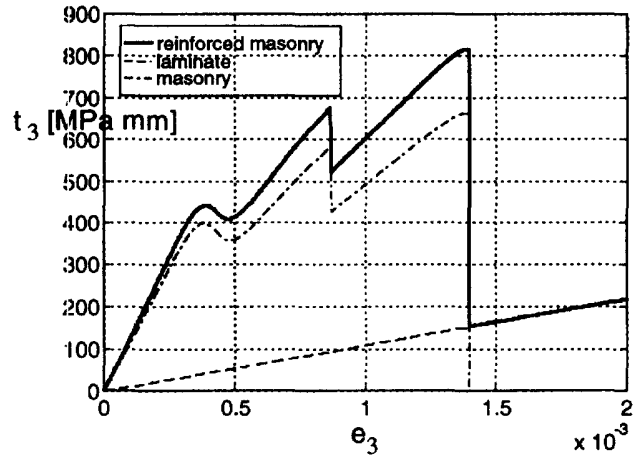

Fig. 11. Average force per unit of length t_3, t_3^M and t_3^l vs average strain e_3 for reinforced masonry.

compression; so, when the reinforced masonry is in tension, the block fails, when it is in compression, the laminate fails. It can be emphasized that this very special behavior of the reinforced masonry can be captured only by performing a micromechanical damage analysis, which also provides the local stretching.

Furthermore, to investigate the phenomenon of the strain concentration a simple sample is studied. It is a reinforced masonry beam, characterized by the unit cell reported in Fig. 12, and subjected to the uniaxial strain $e > 0$. It is set $z = 2a+t = 225$ mm, $c_1 = z/2(a+t) = 0.9375$ and $c_2 = t/2(a+t) = 0.0625$. For this particular scheme, the local strains e^1 and e^2 in the Ω^1 and Ω^2, respectively, are constant. As emphasized above, the mortar is subjected to a strain concentration and, hence, it collapses for low values of the assigned average strain e. Once the mortar is completely damaged, the composite can be considered as made only of blocks and laminae. Therefore, the equation governing the localization of the strains in this composite are:

$$e^1 = \frac{N}{s^M E^b + 2s^r E_L^r}$$

$$e^2 = \frac{N}{2s^r E_L^r}$$

$$e = c_1 e^1 + c_2 e^2 \tag{36}$$

where N is the axial resultant stress in the beam. In particular, eqn (36) gives:

$$e^1 = \frac{\xi}{c_2 + c_1 \xi} e \tag{37}$$

with $\xi = 2s^r E_L^r / s^M E^b$. In Fig. 13 the local strains e^1 and e^2 vs the parameter ξ is plotted for

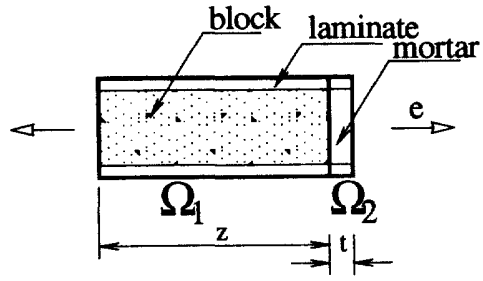

Fig. 12. Simple sample of reinforced masonry subjected to uniaxial strain e.

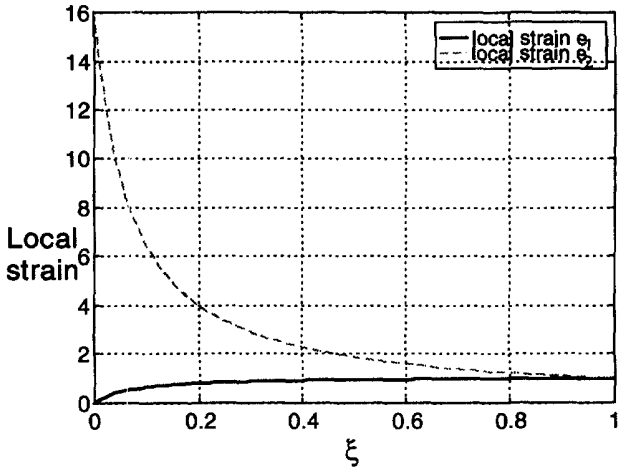

Fig. 13. Local strain e^1 in Ω^1 vs the parameter ξ.

$e = 1$. It can be noted that e^1 is an increasing function of $s^r E_L^r$ and e^2 is a decreasing function of $s^r E_L^r$. Thus, the collapse of the block occurs at a lower value of the average deformation e when a stiffer reinforcement is adopted. As a consequence, the use of too stiff reinforcements leads to a reduction of the average failure strain of the masonry.

An optimal design of the reinforcement should be such that the block does not fail after the laminate. In Fig. 14 the plot of the ratio (stress in Ω^1)/(strength) for the block in tension and in compression and for three laminates characterized by different strengths versus the laminate thickness, is reported for $e = \pm 0.003$. This figure is useful for the determination of the optimal value of the reinforcement thickness. In fact, it can be noted that for $s^r = 2$ mm, the failure of each one of the three possible laminates occurs before the degradation of the block in compression. For $s^r = 8$ mm, the failure of the laminate with strength $\sigma_{lim}^L = 1000$ MPa occurs before the degradation of the block in compression, while the failure of the laminates with strength $\sigma_{lim}^L = 1400$ MPa and $\sigma_{lim}^L = 1800$ MPa occurs after the degradation of the block. Thus, if the laminate with strength $\sigma_{lim}^L = 1800$ MPa is adopted, a thickness greater than 5 mm should be used; analogously, for $\sigma_{lim}^L = 1400$ MPa or $\sigma_{lim}^L = 1000$ MPa, a thickness greater than 7 or 10 mm should be used, respectively.

As a final remark, it can be concluded that the behavior of the reinforced masonry is complex, and the mechanics of the degradation and failure depends on the particular geometry considered, on the elastic properties of the materials, on the strengths of the

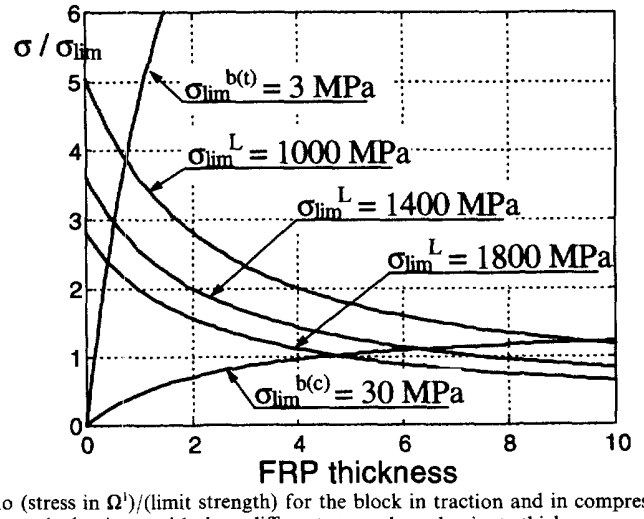

Fig. 14. Ratio (stress in Ω^1)/(limit strength) for the block in traction and in compression and for the laminate with three different strengths vs laminate thickness.

mortar, of the block and of the laminate. The micromechanical approach can account for all these factors.

6. CONCLUSIONS

The reinforced masonry has been regarded as a regular (i.e. periodic) composite material. A simple homogenization technique has been proposed, which allows to compute the strain in the mortar, in the block and in the reinforcement. The damage of the masonry, due to the decay of the mortar and block properties, has been considered. Two different damage criteria have been adopted, one for the mortar and one for the block. Furthermore, for each damage criterion, two evolution laws are presented: a viscoelastic law and an elastic one. A brittle damage model, within the Tsai–Hill failure criterion, is adopted for the laminate. It can be noted that any other kind of damage model for the block, for the mortar and for the laminate can be adopted in the proposed homogenization procedure.

The behavior of unreinforced material has been investigated. Interesting results have been obtained, which emphasize the different behaviour obtained by adopting the viscoelastic or the elastic damage law. Then, numerical applications relative to a reinforced masonry have been developed. Specific effects of this reinforcement on the global behavior of the masonry have been emphasized. These effects can be captured only by performing a micromechanical analysis, which appears to be very recommended for these particular procedures of reinforcement. Furthermore, it can be emphasized that the proposed micromechanical procedure can be properly modified to also account for the debonding effects.

Acknowledgements—The financial support of the Italian National Research Council (CNR) and of the Ministry of University and Research (MURST) are gratefully acknowledged.

REFERENCES

Anthoine, A. (1995) Derivation of the in-plane elastic characteristics of masonry through homogenization theory. *International Journal of Solids and Structures* **32**(2), 137–163.

Barbero, E. J., Luciano, R. and Sacco, E. (1994) Applications of composites in Civil Engineering. In *Advancing with Composites '94*, ed. L. Crivelli Visconti. Woodhead Publishing Limited.

El-Badry, M. (ed.) (1996) *Advanced Composite Materials in Bridges and Structures, 2nd International Conference*, Montréal, Québec, Canada.

Frémond, M. and Nedjar, B. (1996a) Damage in concrete: the unilateral phenomenon. *Nuclear Engineering Design* **156**, 323–335.

Frémond, M. and Nedjar, B. (1996b) Damage, gradient and principle of virtual power. *International Journal of Solids and Structures* **33**(8), 1083–1103.

Gambarotta, L. and Lagomarsino, S. (1994) Damage in brick masonry shear walls. In *Fracture and Damage in Quasibrittle Structures: Experiments, Modelling and Computer Analysis*, eds Z. P. Bazant, Z. Bittnar, M. Jirasek and J. Mazars, pp. 463–472. E & FN SPON (an imprint of Chapman and Hall).

Hilsdorf, H. K. (1969) Investigation into the failure mechanism of brick masonry loaded in axial compression. In *Designing, Engineering and Constructing with Masonry Products*, ed. F. B. Johnson, Proceedings of the International Conference of Masonry Structural Systems, Houston, Texas, pp. 34–41.

Jones, R. M. (1975) *Mechanics of Composite Materials*. Hemisphere Publishing Corporation, New York.

Kralj, B., Pande, G. N. and Middleton, J. (1991) On the mechanics of frost damage to brick masonry. *Computers and Structures* **41**(1), 53–66.

Lemaitre, J. and Chaboche, J.-L. (1990) *Mechanics of Solids Materials*. Cambridge University Press.

Luciano, R. and Sacco, E. (1995) A micromechanical approach to the damage of the masonry material. In *Structural Studies, Repair and Maintenance of Historical Buildings STREMA 95*, eds B. Leftheris and C. A. Brebbia. Computations Mechanics Publications.

Luciano, R. and Sacco, E. (1996) Behavior of masonry panels reinforced with FRP composites. *Proceedings of 2nd International Conference Advanced Composite Materials in Bridges and Structures*, Montréal, Canada.

Luciano, R. and Sacco, E. (1997a) Homogenization technique and damage model for old masonry material. *International Journal of Solids and Structures* **34**(24), 3191–3208.

Luciano, R. and Sacco, E. (1997b) Variational methods for the homogenization of periodic heterogeneous media. *European Journal of Mechanics A/Solids* (submitted).

Machida, A. (ed.) (1993) State-of-the-art report on continuous fiber reinforcing materials. *Japanese Society of Civil Engineers*.

Mazars, J. (1984) Application de la mécanique de l'endommagement au comportement non linéaire et à la rupture du béton de structure. Thèse de Doctorat èn Science, Université de Paris 6.

Mazars, J. and Pijaudier-Cabot, G. (1989) Continuum damage theory. Application to concrete. *Journal of Engineering Mechanics, ASCE* **115**, 345–365.

Meier, U. (1987) Bridge repair with high performance composite materials. *Material and Technik* **4**, 125–128.

Mura, T. (1987) *Micromechanics of Defects in Solids*. Martinus Nijhoff Publishers, New York.

Nanni, A. (ed.) (1993) *Fiber-Reinforced-Plastic Reinforcement for Concrete Structures: Properties and Applications*, Elsevier, Oxford.

Neale, K. W. and Labossière, P. (eds) (1992) *Advanced Composite Materials in Bridges and Structures*, 1*st International Conference*, Sherbrooke, Québec, Canada.

Pande, G. N., Liang, J. X. and Middleton, J. (1989) Equivalent elastic moduli for brick masonry. *Computer & Geotechnics* **8**, 243–265.

Papa, E. (1990) Sulla Meccanica del Danneggiamento con Particolare Riferimento alle Murature. Ph.D. Thesis, Politecnico di Milano, Dipartimento di Ingegneria Strutturale.

Pietruszczak, S. and Niu, X. (1992) A mathematical description of macroscopic behaviour of brick masonry. *Computer & Geotechnics* **29**(5), 531–546.

Schwegler, G. (1994) Masonry construction strengthened with fiber composites in seismically endangered zones. *Proceedings of* 10*th European Conference on Earthquake Engineering*, Vienna, Austria.

Triantafillou, T. C. (1996) Innovative strengthening of masonry monuments with composites. *Proceedings of* 2*nd International Conference Advanced Composite Materials in Bridges and Structures*, Montréal, Canada.

Triantafillou, T. C. and Fardis, M. N. (1993) Advanced composites for strengthening historic structures. *Proceedings of the IABSE Symposium on Structural Preservation of the Architectural Heritage*, Rome, Italy.

Triantafillou, T. C. and Fardis, M. N. (1995) Strengthening of historic masonry structures with fiber reinforced plastic composites. In *Structural Studies, Repair and Maintenance of Historical Buildings STREMA* 95, eds B. Leftheris and C. A. Brebbia. Computational Mechanics Publications.